Supplementary information

Antiretroviral dynamics determines HIV evolution and predicts therapy outcome

Daniel I. S. Rosenbloom[*,1], Alison L. Hill[*,1,2], S. Alireza Rabi[*,3], Robert F. Siliciano[†3,4], and Martin A. Nowak[†1]

[1]Program for Evolutionary Dynamics, Department of Mathematics, Department of Organismic and Evolutionary Biology, Harvard University, Cambridge, MA 02138, USA
[2]Biophysics Program and Harvard-MIT Division of Health Sciences and Technology, Harvard University, Cambridge, MA 02138 USA
[3]Department of Medicine, Johns Hopkins University School of Medicine, Baltimore, MD 21205, USA
[4]Howard Hughes Medical Institute, Baltimore, MD 21205, USA
[*]Authors contributed equally to work
[†]To whom correspondence should be addressed. Email: rsiliciano@jhmi.edu, martin_nowak@harvard.edu

Contents

1 Supplementary Methods **3**

1.1 Viral dynamics model . . . 3

1.2 Model parameters . . . 6

1.2.1 Basic reproductive ratio . . . 6

1.2.2 Latent reservoir exit rate . . . 7

1.2.3 Host cell production rate . . . 8

1.2.4 Resistance mutation rates . . . 8

1.3 Simulation algorithm . . . 10

1.4 Graphing outcome versus adherence . . . 13

1.5 Graphing outcome over time . . . 14

1.6 MSW for combination therapy 14
1.7 Derivation of Fig. 2f: comparing risk of wild type-based and mutant-based VF from selection window data 15

List of Tables

1 Pharmacokinetic and pharmacodynamic parameters for anti-HIV drugs 18
2 Nucleotide substitution rates for HIV 18
3 Parameters for all single-point mutations considered in the study 19
4 Parameters for all single-point mutations considered in the study (Cont'd)[17] 20
5 Pre-existing frequency of mutations and exit rate from the latent reservoir 21
6 Pre-existing frequency and exit rate from the latent reservoir for best "synthetic" mutation for each drug 22
7 Viral dynamics parameters in the absence of drug therapy 22

List of Figures

1 Relative risk of wild type- versus mutant-caused virologic failure for anti-HIV drugs 24
2 Distribution of a) viral load setpoints and b) adherence levels used in simulations . 25
3 Simulated clinical outcomes versus adherence for all drugs, suppression phase . . . 26
4 Simulated clinical outcomes versus adherence for all drugs, maintenance phase . . 27
5 Simulated clinical outcomes versus time for all drugs, suppression phase 28
6 Simulated clinical outcomes versus time for all drugs, maintenance phase 29
7 Simulated clinical outcomes versus time for all drugs, maintenance phase allowing recovery 30

8 Simulated clinical outcomes versus adherence for all drugs, pre-existing vs. *de novo* mutations in suppression phase 31
9 Simulated clinical outcomes versus adherence for all drugs, pre-existing vs. *de novo* mutations in maintenance phase 32
10 Simulated clinical outcomes versus adherence for all drugs, R_{00}=20 33
11 Simulated clinical outcomes versus adherence for all drugs, R_{00}=5 34
12 Simulated clinical outcomes versus adherence for NRTIs with large inter-experimental variation in half-life 35
13 Selection regimes for two-drug therapy 36

1 Supplementary Methods

1.1 Viral dynamics model

The following system of equations models the dynamics of multiple strains ($i = 1, 2, \ldots, n$) of HIV in a patient:

$$\begin{aligned} \dot{x} &= \lambda - \sum_{i=1}^{n} \beta_i x v_i - d_x x \\ \dot{y}_i &= \beta_i x v_i + A_i - d_y y_i \\ \dot{v}_i &= k_i y_i - d_v v_i \end{aligned} \tag{1}$$

where state variables x, y_i, and v_i are the number of infectable $CD4^+$T-cells, the number of actively infected cells of strain i, and the number of free virus particles of strain i, respectively. The number of latently infected cells is considered to be constant, as it doesn't decay significantly over the course of a clinical trial, and so latently infected cells of strain i activate at a constant rate A_i. Active cells produce virus at rate k_i and die at rate d_y, and virus is cleared at rate d_v. The infectivity

parameter β_i determines the rate at which virus of strain i infects susceptible host cells. Host cell dynamics are determined by production rate λ and death rate d_x.

When $A_i = 0$ for a strain i, this model reduces to the traditional viral dynamics model[14]. For that model we can describe the *basic reproductive ratio*, which is defined as the number of new infections generated by a lone infected cell before it dies. Strain i will only have a positive growth rate and be capable of sustaining an infection if its basic reproductive ratio, $R_{0i} := \lambda\beta_i k_i / \left(d_x d_y d_v\right)$, is greater than 1. In the model we present here the latent reservoir provides a constant source of virus (A_i), which removes the threshold criteria for R_0, although this value still describes viral fitness and the amount of ongoing viral replication.

For a single strain, the unique non-negative steady-state solution to our model is

$$y_1 = \frac{\lambda}{2d_y R_{01}}\left[R_{01}\left(\frac{A_1}{\lambda}+1\right) - 1 + \sqrt{R_{01}^2\left(\frac{A_1}{\lambda}+1\right)^2 + 2R_{01}\left(\frac{A_1}{\lambda}-1\right)+1}\right] \tag{2}$$

In our model, for $R_{0i} > 1$, strain i grows to a high steady state that depends on availability of host cells and the abundance of other strains. There are several limiting cases that can be derived from equation (2). In the absence of other strains (or if $R_{0j} \ll 1$ for all $j \neq i$), and for small reactivation $A_i \ll \lambda$, strain i grows to the steady state $y_i \approx \tilde{Y}_i := \lambda\left(R_{0i}-1\right) / \left(d_y R_{0i}\right)$. The value $\tilde{Y}_i$ is the setpoint viral load that is maintained by replication alone, without additional contribution from the latent reservoir. The residual active infection maintained by the latent reservoir in complete absence of viral replication ($R_{0i} = 0$) is $\tilde{y}_{0i} := A_i/d_y$. For positive $R_{0i} < 1$, strain i reaches a low steady state $y_i \approx \tilde{y}_i := \tilde{y}_{0i}/\left(1 - R_{0i}\right)$. Since anti-HIV drugs act by decreasing β_i and k_i, the value of R_{0i} is understood to depend on the current drug concentration(s).

To eliminate some of the model parameters and smooth the high-frequency fluctuations that

may have little clinical impact over the course of a drug trial, we study a simplified version of the model in Equation (1). We assume that v_i and x are at equilibrium relative to y_i. This allows us to derive a reduced n-dimensional model:

$$\dot{y}_i = A_i + d_y y_i \left[\frac{\lambda R_{0i}}{\lambda + \sum_{j=1}^{n} R_{0j} d_y y_j} - 1 \right] \tag{3}$$

When the total infection is small, the summation term vanishes, and $\dot{y}_i \approx A_i + d_y y_i (R_{0i} - 1)$. For $R_{0i} \ll 1$, nearly all of strain i is produced by exit from the reservoir; y_i therefore approaches a value near $\tilde{y}_{0i}$. As the total infection grows (assuming $R_{0i} > 1$ for one or more i), the fractional term approaches 1, describing saturation of the limiting resource, at which point new infection events are balanced precisely by death of infected cells and y_i approaches a value near $\tilde{Y}_i$. This reduced model has identical steady state values of virus and $CD4^+$cells as the full model, but smooths out fluctuations in infection size caused by the dynamics of total $CD4^+$cells. Because we focus on initial virologic failure, which occurs at relatively low viral loads, the fluctuations in $CD4^+$cell levels are minor, and the approximation captures the full dynamics (1) well.

We can account for mutation by including the mutation rate matrix Q, where Q_{ij} describes the probability that an infected cell of type j gives rise to one of type i:

$$\dot{y}_i = A_i + \frac{\lambda d_y \sum_{j=1}^{n} y_j R_{0j} Q_{ij}}{\lambda + \sum_{j=1}^{n} R_{0j} d_y y_j} - d_y y_i \tag{4}$$

$$\tag{5}$$

1.2 Model parameters

The value of R_{0i} at each point in time depends on the baseline basic reproductive ratio ($R_{00} = 10$, see below), the current drug concentration(s), and parameters describing resistance of the strain, as described by Equations 1 and 2 in the main text. The death rate of actively infected cells, d_y, is 1 per day[66]. Suppl. Table 7 summarizes the parameters used in the model.

1.2.1 Basic reproductive ratio

The basic reproductive ratio (R_0) combines various components of viral fitness into a single number. $R_0 > 1$ is required for the virus to have a positive growth rate and sustain an infection. The baseline R_0, which we denote R_{00}, is defined in the absence of drug and has been estimated in past studies by measuring the increase in viral load during the early days of acute infection or during planned treatment interruption. During the acute phase, before the CTL response develops, typical values for R_{00} are 10-20[63; 67]. After this initial phase, R_{00} declines to 2-5, with some outliers as high as 6-11[68–72]. Based on these findings, we chose a value of R_{00}=10 to present our results. We also checked sensitivity to this parameter by using larger and smaller R_{00} values (Suppl. Fig. 10) and 11).

We can also double-check that our value of R_{00} from the literature is consistent with an independent set of measurements. The growth rate of a mutant strain in the absence of drug is $R_{00} * (1 - s)$ (see Equation 1 in the main text), where s is the reduction in the replication capacity of the mutant virus. If $R_{00} * (1 - s) > 1$, then a mutant strain will expand in the absence of drug. If this condition fails, then the mutant strain would never be detected at high abundance (ignoring secondary or compensatory mutations). Since all the resistance mutations that we study do occur clinically, we expect that $R_{00} > 1/(1 - s)$ should almost always hold. 95% of the mutations studied have $s < 0.9$, for which the positive growth condition is satisfied for the value $R_{00} = 10$.

To maintain consistency with the chosen value $R_{00} = 10$, we capped the cost of mutations used in the viral dynamics simulation at $s = 0.9$, guaranteeing that no mutant's baseline R_0 would be less than 1. Values of s that are negative are also inappropriate for our model, as they imply that the resistant mutant is more fit than the wild type even in the absence of the drug, causing the mutant to be prevalent at baseline. Measurements of s that were close to 0 or negative were assumed to be caused by experimental error, and so we set these values to $s = 0.05$ to represent a small cost to these mutations.

1.2.2 Latent reservoir exit rate

Based on the following argument, we estimate the total reservoir exit rate $\sum_i A_i$ to be 3000 cells per day. The exit rate for a particular mutant strain is determined by multiplying by the equilibrium frequency of pre-existing mutants, u/s. (Our simulation treats each exit as an independent event; use of this modeling approach implicitly assumes that the reservoir was seeded by a large, diverse population, and that its diversity, or effective population size, is maintained over time.) Viral loads of around 2 RNA copies/mL are maintained in patients on maximally suppressive HAART[73]. The rate of exit from the reservoir must be enough to account for this residual viral load, since ongoing replication is negligible. This viral load corresponds to $\approx 3 \times 10^3$ plasma virions (for a 70 kg person with 3L plasma). It has been shown, for a wide range of viral loads, that the total number of infected cells in a patient is roughly equal to the number of plasma virions[74]. The infection size $\sum y_i \approx (\sum A_i)/d_y$ is therefore 3×10^3, implying a total reservoir exit rate of 3000 cells per day.

Alternately, we can estimate the number of infected cells by noting that total viral production (burst from infected cells) must balance total viral clearance (breakdown of free virus in lymphatic tissue). Using parameters established in[75], free virus in lymph tissues is 100 times as abundant as virus in the extracellular fluid, and so would be about 1.5×10^6 virions (based on 15L ECF) for

this example. This paper also determined that the ratio of viral burst size to viral clearance rate is typically 500 virions per cell (e.g., k_i = 10,000 virions per day per cell; d_v = 20 per day). These figures again imply an infection size of 3000 cells.

Our calculations also agree with the results of a model which examined the many years-long decay of the latent reservoir in HAART patients[76]. Although this model used different sources for parameter values, it is consistent with an exit rate of 3000 cells per day, as long as the reservoir is not significantly depleted.

1.2.3 Host cell production rate

For a single wild-type strain in the absence of drug, the model (3) provides $\lambda = \tilde{Y} d_y R_{00} / (R_{00} - 1)$, where $\tilde{Y}$ is the total number of infected cells at infection setpoint. As established above, this value is approximately equal to the number of plasma virions at setpoint. We considered setpoint viral loads from 3000 to 10^6 RNA copies per ml plasma, or 4.5×10^6 to 1.5×10^9 total plasma virions. These values give a range of 5×10^6 to 1.7×10^9 cells per day for λ.

1.2.4 Resistance mutation rates

The mutation rate matrix entry Q_{ij} describes the probability that strain j reproduces to create strain i. We include only single step mutations from the wild type ($j = 1$) to another strain i (at rate u_i) and ignore back-mutation. Therefore $Q_{i1} = u_i$ for $i > 1$, $Q_{1,1} = 1 - \sum_{k=2}^{n} u_k$, $Q_{ii} = 1$ for $i > 1$ and $Q_{ij} = 0$ for all other entries.

The overall mutation rate for HIV is 3×10^{-5} per base per replication cycle[77], and recent work has shown that the rate varies considerably depending on the specific base changes involved. The nucleotide mutation matrix used in this study was derived by normalizing mutation accumulation data from a study of HIV replication of lacZα reporter sequence[78]. The normalized data was

then rescaled to convert from the lacZα base composition to the HIV consensus sequence base composition[79]. Specifically:

1. Define the variables:

   - $u = 3 \times 10^{-5}$ is the average per-site mutation rate of HIV.
   - s_{xy} is the total number of single-nucleotide substitutions from base x to base y, combining data from both the forward and reverse orientations of lacZα in Table 3A of Abram et al.[78].
   - s_{x*} is the total number of single-nucleotide substitutions from base x to any other base.
   - S is the total number of single-nucleotide substitutions overall.
   - n_x and n'_x are the abundance of base x in the reporter sequence and in the HIV consensus sequence, respectively. N and N' are the lengths of the two sequences, respectively.
     - $n_T = 37, n_C = 56, n_A = 36, n_G = 45; N = 174$
     - $n'_T = 2163, n'_C = 1772, n'_A = 3411, n'_G = 2373; N' = 9719$

2. Calculate the relative mutability of each base x in the reporter sequence, $r_x = (s_{x*}/n_x) \,/\, (S/N)$. A value $r_x > 1$ indicates that base x is more mutable than the average, while $r_x < 1$ indicates the opposite.

3. The per-site mutation rates from all bases x, denoted u_{x*}, are assumed to be proportional to the relative mutabilities r_x. To compute the values u_{x*}, scale the relative mutabilities so that the sum $n'_T u_{T*} + n'_C u_{C*} + n'_A u_{A*} + n'_G u_{G*}$ equals $N'u$, the genomic mutation rate of HIV (about 0.3 substitutions per replication). The correct scaling factor is $u_{x*}/r_x = N'u/\left(\sum r_x n'_x\right)$.

4. To determine the individual rates u_{xy}, partition each value u_{x*} proportional to the substitutions counted in the reported sequence; that is, $u_{xy} = u_{x*}\left(s_{xy}/s_{x*}\right)$.

Suppl. Table 2 gives the resulting per-site probability (u_{xy}) for each nucleotide substitution in a single round of viral replication.

Mutation rates were calculated only for those amino acid substitutions which could be achieved via a single nucleotide change. All drugs studied had at least one such substitution that conferred resistance. For each possible starting codon, the rate of substitution equals the sum of all rates of nucleotide substitutions that achieve the desired amino acid change. The mutation rate u then equals the average of rates for all possible starting codons, weighted by the probability of finding that codon (based on the HIV consensus sequence base composition) (used in Suppl. Table 5, 6).

1.3 Simulation algorithm

We used stochastic simulations to study the dynamics of the system described in (3) with mutation. Multiple mutations have been characterized for each drug, and to model a realistic worst-case scenario, we considered a single "synthetic" mutant defined as having the highest benefits (ρ, negative σ), lowest cost (s), and highest mutation rate of all the single-nucleotide mutants known for that drug. Each monotherapy simulation therefore tracked only two strains, wild type y_1 and mutant y_2. Simulations modeled 48-week trials, using discrete timesteps of $\Delta t = 30$ minutes. All simulations were done in Matlab R2010b. The following steps describe the simulation for a single patient on monotherapy, with expected adherence value α:

1. Draw from the viral load setpoint distribution in Suppl. Fig. 2a. This setpoint is used to determine the value of the λ parameter, assuming that the patient has 3 L plasma.

    - In the suppression phase of therapy, the initial infection size is the setpoint, rounded to the nearest integer number of cells.
    - In the maintenance phase of therapy, the initial infection size is the fully-suppressed infection size $\sum y_i \approx (\sum A_i)/d_y = 2$ c/ml.

2. Assign each infected cell to the mutant population (y_2) with probability u/s; otherwise the cell is in the wild-type population (y_1).

3. Identify all scheduled doses for the entire trial. All scheduled doses are evenly spaced, with the first dose occurring at the beginning of the trial. The patient takes each scheduled dose with probability α.

    - Exception: in the maintenance phase, the patient is always assumed to take the first scheduled dose.

4. Calculate the drug concentration every timestep, as described in Methods.

    - In the suppression phase, the initial drug concentration is zero.
    - In the maintenance phase, the initial drug concentration is C_{max}.

5. Calculate the basic reproductive ratios for the wild type and the mutant every timestep, as described in Equations 1 and 2 of the main text and the Methods.

6. For each timestep:

    (a) The number of infected cells of strain i to exit the reservoir is drawn from a Poisson distribution with mean value $A_i \Delta t$.

    (b) The number of newly infected cells generated by strain i is drawn from a Poisson distribution with mean value $d_y y_i \Delta t \left[\frac{\lambda R_{0i}}{\lambda + \sum_{j=1}^{n} R_{0j} d_y y_j} \right]$.

    (c) Each cell newly infected by the wild type enters the mutant population with probability u; otherwise it remains wild type. Cells infected by the mutant do not back-mutate.

    (d) Each infected cell dies with probability $1 - \exp(-d_y \Delta t)$.

7. Determining outcome at 48 weeks:

- In the suppression phase, the patient's status is observed at the end of the 48-week trial. If viral load is below 50 c/ml, the trial is declared successful; otherwise virologic failure occurs.
- In the maintenance phase, the patient's status is observed each week for 48 weeks, beginning at week 5. If any two consecutive observations show a viral load of at least 200 c/ml, virologic failure occurs; otherwise the trial succeeds.
- A failed trial is considered a mutant-based failure if at least 20% of the viral population is mutant; otherwise it is considered a wild type-based failure.

8. Determining outcome over time:

   - Patient's status was evaluated every 2 weeks, for 48 weeks.
   - In the suppression phase, if viral load is below 50 c/ml at the evaluation, the patient is classified as having "suppressed viral load;" otherwise the patient has "detectable viral load."
   - In the maintenance phase, the patient's viral load is measured each week for 48 weeks, beginning at week 5. If any two consecutive measurements at or before the evaluation show a viral load of at least 200 c/ml, the patient is declared to have "detectable viral load," and is then removed from the trial, retaining this classification for all future time-points. Otherwise, the patient is declared to have "suppressed viral load."
   - In the maintenance phase allowing recovery, the patient's viral load is measured as in the maintenance phase above. If viral load is at least 200 c/ml both at the evaluation and at the immediately preceding measurement, the patient is declared to have "detectable viral load." Patients who were previously "detectable" remain in the trial and may re-suppress.
   - A measurement of "detectable viral load" is considered "via resistance" if at least 20%

of the viral population is mutant; otherwise it is considered to be "via wild type."

By using a well-mixed population and by assuming that the processes of reservoir exit, replication, and death are Poisson, this method implicitly sets the effective population size of the infection equal to the census size of infected cells. Population structure, selection on linked loci, and variations in burst size among infected cells are all mechanisms that could increase variance in viral offspring number, decreasing the effective population size[80;81]. Estimating the relevant population size to use for a model of drug resistance is difficult, as most approaches define an effective population size only for neutral loci. Simply "plugging in" a population size derived from a model without selection would be misleading in this context[82], and in lieu of a more informed value, we simply use the census size. This approach likely overestimates probabilities of mutant emergence and underestimates variability among patients[83;84].

For dual therapy, we consider three strains: wild type, resistant to drug 1, resistant to drug 2. The two drugs can be simulated as two separate pills (allowing each pill to be taken or forgotten independently) or as a single combination pill (forcing the two drug concentrations to rise and fall in lockstep). In the case of two separate pills, the value of α may be different for each drug, allowing for "differential adherence" – which has been observed in some studies[35].

1.4 Graphing outcome versus adherence

For each monotherapy, 25,250 patients were simulated, with expected adherence α ranging from 0 to 1 (roughly equal numbers of patients were simulated for each 1% increment, including 50 patients with $\alpha = 0$ and 50 patients with $\alpha = 1$). The x-axis measures the *ex post* adherence for patients — that is, the actual percentage of doses taken, which may differ from the expectation α. Results were plotted for overlapping 2% windows, centered every 1% between 0 and 1, as well as for the points 0 and 1 themselves.

Analysis of dual therapy with a combination pill was similar to that of monotherapy, but with 126,250 patients (including 250 patients with $\alpha = 0$ and 250 patients with $\alpha = 1$).

For dual therapy with separate pills, 169,000 patients were simulated, with expected adherences α_1, α_2 ranging from 0 to 1 (roughly equal numbers of patients were simulated for each 4% × 4% increment, including 25,000 patients on the border of the distribution where at least one α_i is equal to 0 or 1.) As with monotherapy, the axes measure *ex post* adherence. Results were plotted for overlapping 4% × 4% windows, centered every 2% between 0 and 1; points plotted on the border of the distribution show patients with at least one α_i exactly equal to 0 or 1.

Note that, for maintenance therapy, the axes do not include zero, as each patient is guaranteed to take the first dose (adherence is never zero).

1.5 Graphing outcome over time

Analysis was performed separately for each overlapping 2% adherence window, centered every 1% between 0 and 1, as well as for the points 0 and 1 themselves. The resulting graph shows a weighted average of these results, using the adherence distribution in Suppl. Fig. 2. Measurements were taken every two weeks, and the graphs show the proportion of the population with each outcome. As there is no censoring of data, the analysis is equivalent to the Kaplan-Meier method[85].

1.6 MSW for combination therapy

For calculations involving combination therapy (limited to two drugs in this paper), viral fitness is influenced by the dose-response curves of all drugs. DRV and RAL belong to different classes and have been shown to reduce fitness in a multiplicative (Bliss-independent) fashion, which is often

expected for drugs acting on different targets [27;28]. The equation describing viral fitness with two Bliss-independent drugs is given by:

$$R_0(D_1, D_2) = \frac{R_{00}}{\left(1 + \left(\frac{D_1}{IC_{50,1}}\right)^{m_1}\right)\left(1 + \left(\frac{D_2}{IC_{50,2}}\right)^{m_2}\right)} \tag{6}$$

where D_1, D_2 are the concentrations of each drug in the relevant compartment, $IC_{50,1}, IC_{50,2}$ are the concentrations at which 50% inhibition occurs, and m_1, m_2 are the slope parameters. The numerator R_{00} is the baseline basic reproductive ratio in the absence of drug treatment. Mutations that confer resistance to a given drug change the IC_{50}, slope and drug-free fitness similarly to the way described in Equation 2 (main text).

For a two-drug combination where we assume that a viral strain may only be resistant to a single drug, there are now eight potential selection windows. Drug levels may be high enough for guaranteed treatment success; in the MSW for one or both drugs; in the overlapping region for one or both of the MSWs and the WGW, or strictly in the WGW. Suppl. Fig. 13 shows the possible windows for the RAL+DRV/r combination.

1.7 Derivation of Fig. 2f: comparing risk of wild type-based and mutant-based VF from selection window data

Fig. 2f in the main text ranks drugs by the relative risk of mutant versus wild-type failure, regardless of the total risk of failure, based on the time spent in each selection window. The ranks are plotted along a line with values ranging from -1 (DRV/r and d4T, highest relative risk of wild-type failure) to 1 (FTC, the highest relative risk of mutant failure). This plot was constructed based on the data in Fig. 2a in the main text. To devise this scale, we let

x = time until entry into MSW (days) / time until entry into WGW (days)

= length of green bar / length of green + dark red bars,

(7)

y = time spent in MSW (days)

= length of both red bars.

If the drug immediately enters the WGW at day 0, or if it skips the MSW completely, then x is defined to be 1.

Then the scale value to be plotted, a, is calculated as

$$a = \frac{y}{y_{max}} - x, \tag{8}$$

where $y_{max} \approx 16.5$ days, the maximum time that a drug spends in the MSW (obtained for FTC). Since both x and y/y_{max} range between 0 and 1, the scale ranges between -1 (failure via wild type only) and 1 (largest relative risk of resistance).

In this formula, x is a proxy for the rapidity of wild type-caused virologic failure ("wild-type risk") relative to mutant-caused virologic failure ("mutant risk"). When x is small, the MSW window is reached long before the WGW, meaning that "mutant risk" is high and "wild-type risk" is low. When x is high, the WGW is reached soon after the MSW, or without ever entering the MSW, and so "wild-type risk" is high and "mutant risk" is low. While x considers how quickly the infection can start to grow, it does not consider the length of time in the MSW. Even if the MSW begins as soon as a dose is taken (so that $x = 0$), one still needs to consider for how long the mutant strain is selected over the wild-type to determine whether mutant-based or wild type-based virologic failure is more likely to occur. Fig. 1 shows a scatter plot of y versus x.

Supplementary Tables

Table 1: Pharmacokinetic and pharmacodynamic parameters for anti-HIV drugs used in the study[17]

Class	Drug	IC_{50} (μMol)	slope	C_{max} (μMol)	half-life (hrs)	dosing (d^{-1})
NRTI	3TC	0.0298	1.15	15.3	10.0	2
	ABC	0.0381	0.93	10.5	21.0	2
	AZT	0.1823	0.85	4.5	8.5	2
	d4T	0.5524	1.13	2.3	3.5	2
	ddI	0.1795	1.07	39.4	18.0	1
	FTC	0.0079	1.20	7.3	39.0	1
	TDF	0.0561	0.97	1.1	60.0	1
NNRTI	EFV	0.0035	1.69	12.9	35.8	1
	ETV	0.0050	1.75	1.6	41	2
	NVP	0.0490	1.49	25.2	21.5	1
PI	ATV	0.0150	2.90	3.3	6.5	1
	ATV/r	0.0150	2.90	6.3	8.6	1
	DRV/r	0.0265	3.55	14.8	15.0	2
	IDV	0.0550	4.5	10.9	1.8	3
	IDV/r	0.0550	4.5	12.5	3.5	2
	LPV/r	0.0380	2.1	15.6	9.9	2
	NFV	0.2360	1.88	5.1	4.0	3
	SQV	0.0550	3.74	3.1	4.3	3
	SQV/r*	0.0550	3.74	7.9	4.3	2
	TPV/r	0.2500	2.55	77.6	6.0	2
II	EVG	0.0280	0.94	1.7	8.6	1
	RAL	0.0150	1.03	4.0	10.0	2
FI	ENF	0.0349	1.60	1.1	3.8	2

Table 2: Each entry gives the per-site transition probability from row base to column base in one round of viral replication. For derivation and source see Section 1.2.4. The extraordinary skew of this matrix (the largest entry, G-to-A mutation, is more than 300 times the smallest, C-to-G mutation) reflects the base composition of the genome, particularly the bias towards A. Values less than 10^{-6} are particularly uncertain, as they were computed from fewer than 5 substitution observations each.

	U	C	A	G
U		1.1×10^{-5}	1.3×10^{-5}	3.6×10^{-6}
C	2.4×10^{-5}		6.5×10^{-6}	1.7×10^{-7}
A	7.9×10^{-7}	5.3×10^{-7}		1.1×10^{-5}
G	8.5×10^{-7}	8.5×10^{-7}	5.5×10^{-5}	

Table 3: Parameters for all single-point mutations considered in the study[17]

Class	Mutation	Cost (s)	u	Drug	ρ	σ
NRTI	K65R	0.41	1.1×10^{-5}	3TC	61	-0.19
				ABC	47	0.01
				ddI	20	-0.09
				FTC	29	-0.04
				TDF	43	0.00
	M184V	0.46	1.1×10^{-5}	3TC	963	-0.58
				ABC	9.5	-0.44
				AZT	0.28	-0.03
				ddI	9.5	-0.21
				FTC	1186	-0.49
				TDF	3.0	-0.27
	M41L	0.17	1.3×10^{-6}	AZT	2.2	0.07
				d4T	1.0	0.07
	T215Y	0.05	*	AZT	3.1	-0.34
				d4T	1.08	-0.12
NNRTI	G190S	0.79	2.2×10^{-5}	EFV	70	-0.40
				NVP	237	-0.34
	K101P	0.7	*	ETV	5.00	-0.27
	K103N	0.3	1.5×10^{-6}	EFV	85	-0.17
				NVP	94	-0.15
	Y181C	0.26	1.1×10^{-5}	EFV	2.6	-0.11
				ETV	11	-0.26
				NVP	234	-0.40
	Y181I	0.44	*	ETV	100	-0.37
				NVP	1309	-0.50

* Indicates mutation that requires two nucleotide changes;
mutation rate depends on prevalence of intermediate states.

Table 4: Parameters for all single-point mutations considered in the study (Cont'd)[17]

Class	Mutation	Cost (s)	u	Drug	ρ	σ
PI	D30N	0.27	5.5×10^{-5}	NFV	2.3	-0.29
	G48V	0.45	8.5×10^{-7}	SQV	2.0	-0.23
	I47A	0.9	*	LPV	5.8	-0.40
	I47V	0.05	1.1×10^{-5}	LPV	1.8	-0.29
	I50L	0.75	9.0×10^{-7}	ATV	1.2	-0.34
	I50V	0.93	1.1×10^{-5}	DRV	0.68	-0.07
	I54L	0.05	9.0×10^{-7}	DRV	0.98	-0.01
	I84V	0.82	1.1×10^{-5}	ATV	0.60	-0.34
				DRV	0.94	-0.01
				IDV	0.73	-0.39
				TPV	0.26	-0.39
	L33F	0.49	6.3×10^{-6}	TPV	1.4	0.02
	L90M	0.30	3.2×10^{-6}	NFV	1.5	0.01
				SQV	1.1	-0.28
	M46I	0.05	5.6×10^{-5}	IDV	1.0	-0.29
	M46L	0.05	1.3×10^{-6}	IDV	0.76	-0.24
	N88S	0.55	1.1×10^{-5}	ATV	3.1	-0.31
	V32I	0.09	4.1×10^{-5}	LPV	0.53	-0.16
	V82A	0.59	1.1×10^{-5}	LPV	1.03	-0.33
	V82F	0.79	3.4×10^{-7}	IDV	0.89	-0.58
				LPV	1.45	-0.44
	V82T	0.22	*	IDV	0.98	-0.34
				LPV	0.87	-0.17
				TPV	0.68	-0.20
II	G140S	0.71	2.2×10^{-5}	RAL	2.1	0.03
	N155H	0.55	5.3×10^{-7}	EVG	20	0.00
				RAL	27	0.02
	Q148H	0.73	2.0×10^{-6}	EVG	6.8	-0.04
				RAL	86	0.06
	Q148K	0.76	6.5×10^{-6}	EVG	19	0.03
				RAL	128	-0.06
	Q148R	0.61	1.1×10^{-5}	EVG	68	0.06
				RAL	90	0.04
	Y143C	0.74	1.1×10^{-5}	RAL	3.6	0.06
	Y143H	0.55	1.1×10^{-5}	RAL	2.7	-0.04
	Y143R	0.32	*	RAL	75	-0.01
FI	G36D	0.12	2.2×10^{-5}	ENF	1.7	-0.45
	N42T	0.54	5.3×10^{-7}	ENF	2.9	-0.13
	N43D	0.88	1.1×10^{-5}	ENF	13	-0.06
	Q40H	0.26	1.5×10^{-6}	ENF	12	-0.31
	V38A	0.17	1.1×10^{-5}	ENF	11	-0.32

* Indicates mutation that requires two nucleotide changes;
mutation rate depends on prevalence of intermediate states.

Table 5: Pre-existing frequency of mutations and exit rate from the latent reservoir

class	mutation	equilibrium frequency	reservoir exit (days)
NRTI	K65R	2.7×10^{-5}	12
	M184V	2.4×10^{-5}	14
	M41L	7.8×10^{-6}	43
	T215Y	*	*
NNRTI	G190S	2.8×10^{-5}	12
	K101P	*	*
	K103N	4.9×10^{-6}	68
	Y181C	4.3×10^{-5}	8
	Y181I	*	*
PI	D30N	2.0×10^{-4}	2
	G48V	1.9×10^{-6}	177
	I47A	*	*
	I47V	2.2×10^{-4}	2
	I50L	1.2×10^{-6}	279
	I50V	1.2×10^{-5}	28
	I54L	1.8×10^{-5}	19
	I84V	1.4×10^{-5}	25
	L33F	1.3×10^{-5}	26
	L90M	1.1×10^{-5}	31
	M46I	1.1×10^{-3}	< 0.5
	M46L	2.6×10^{-5}	13
	N88S	2.0×10^{-5}	17
	V32I	4.6×10^{-4}	1
	V82A	1.9×10^{-5}	18
	V82F	4.3×10^{-7}	769
	V82T	*	*
II	G140S	3.1×10^{-5}	11
	N155H	9.6×10^{-7}	349
	Q148H	2.0×10^{-6}	166
	Q148K	8.5×10^{-6}	39
	Q148R	1.8×10^{-5}	18
	Y143C	1.5×10^{-5}	22
	Y143H	2.0×10^{-5}	17
	Y143R	*	*
FI	G36D	1.8×10^{-4}	2
	N42T	9.8×10^{-7}	342
	N43D	1.3×10^{-5}	27
	Q40H	5.6×10^{-6}	59
	V38A	6.5×10^{-5}	5

* Indicates mutation that requires two nucleotide changes;
equilibrium frequency depends on prevalence of intermediate states.

Table 6: Pre-existing frequency and exit rate from the latent reservoir for best "synthetic" mutation for each drug

class	drug	equilibrium frequency	reservoir exit (days)
NRTI	AZT	2.4×10^{-5}	14
	d4T	7.8×10^{-6}	43
	3TC	2.7×10^{-5}	12
	FTC	2.7×10^{-5}	12
	ABC	2.7×10^{-5}	12
	ddI	2.7×10^{-5}	12
	TDF	2.7×10^{-5}	12
NNRTI	EFV	4.3×10^{-5}	8
	NVP	4.3×10^{-5}	8
	ETV	4.3×10^{-5}	8
PI	DRV	1.8×10^{-5}	19
	NFV	2.0×10^{-4}	2
	SQV	1.1×10^{-5}	31
	LPV	4.6×10^{-4}	1
	ATV	2.0×10^{-5}	17
	IDV	1.1×10^{-3}	< 0.5
	TPV	1.4×10^{-5}	25
II	RAL	3.1×10^{-5}	11
	EVG	1.8×10^{-5}	18
FI	ENF	1.8×10^{-4}	2

Table 7: Viral dynamics parameters in the absence of drug therapy

	Parameter	Value	Units	Reference
R_{00}	Baseline basic reproduction ratio	10	(unitless)	See text
d_y	Death rate of actively infected cells	1	d^{-1}	[66]
v_0	Residual plasma viral load maintained by activation from latent reservoir, absent viral replication	2	RNA copies / ml plasma	[73]
A	Latent reservoir exit rate	3000	cells / d	Based on v_0, see text

Supplementary Figures

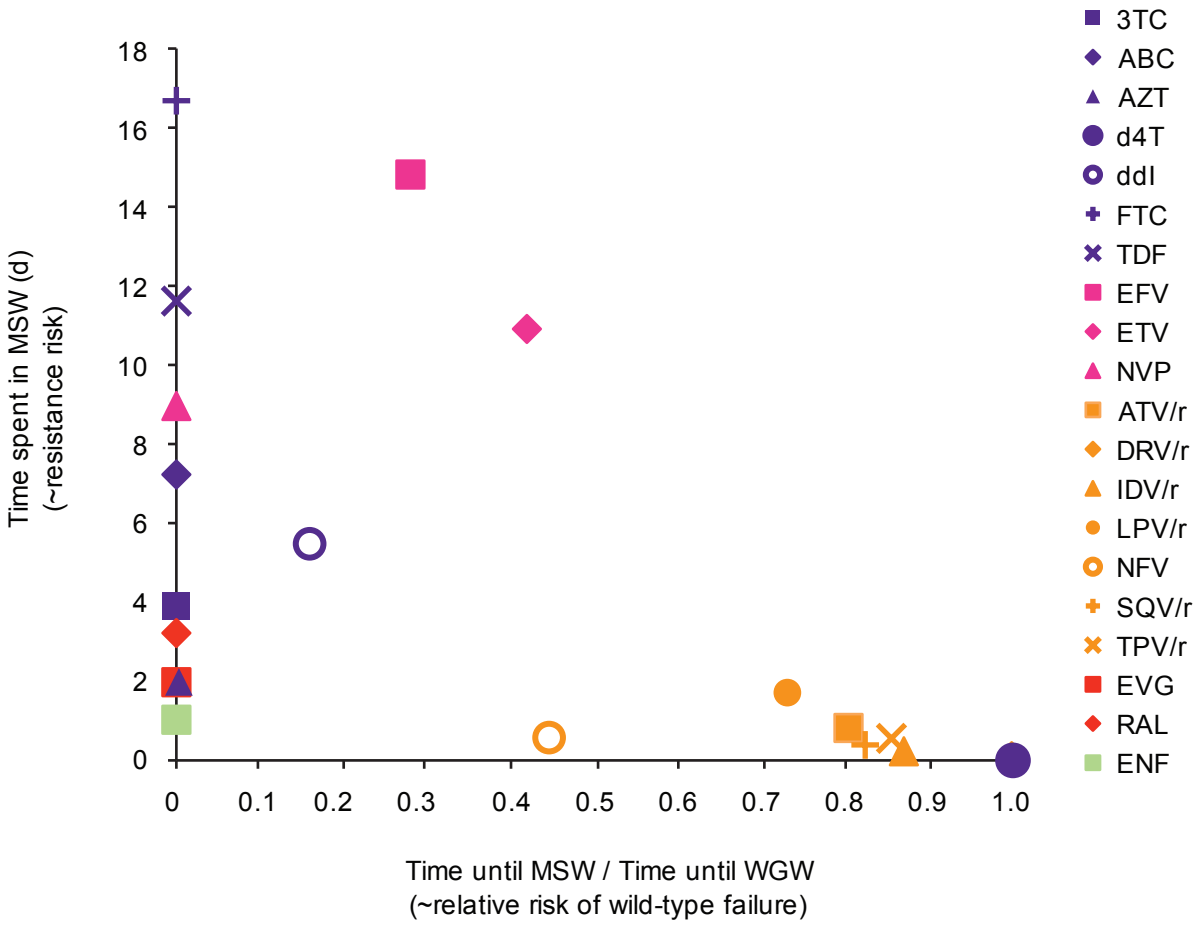

Figure 1: Relative risk of wild type- vs. mutant-caused virologic failure for anti-HIV drugs, considering the best "synthetic" mutation defined in Section 1.3. Two metrics can be used to compare the risk of resistance to the likelihood of wild-type growth, shown on both axes. The x-axis measures the time until a patient interrupting treatment reaches the MSW, divided by the time until that patient reaches the WGW. The y-axis measures the number of days that a patient spends in the MSW during a treatment interruption. Drugs tend to cluster near the endpoints of the x-axis: most NRTIs, the IIs, and the FI are on the left, meaning that the patient enters the MSW immediately or soon after interruption, and most PIs are on the right, meaning that the patient waits relatively long to enter the MSW. Section 1.7 further describes the two metrics and explains how they were used in Fig. 2f in the main text to rank the drugs by relative risk of mutant-based versus wild type-based VF. Note that the symbol for DRV/r is obscured behind the symbol for d4T at $(1, 0)$.

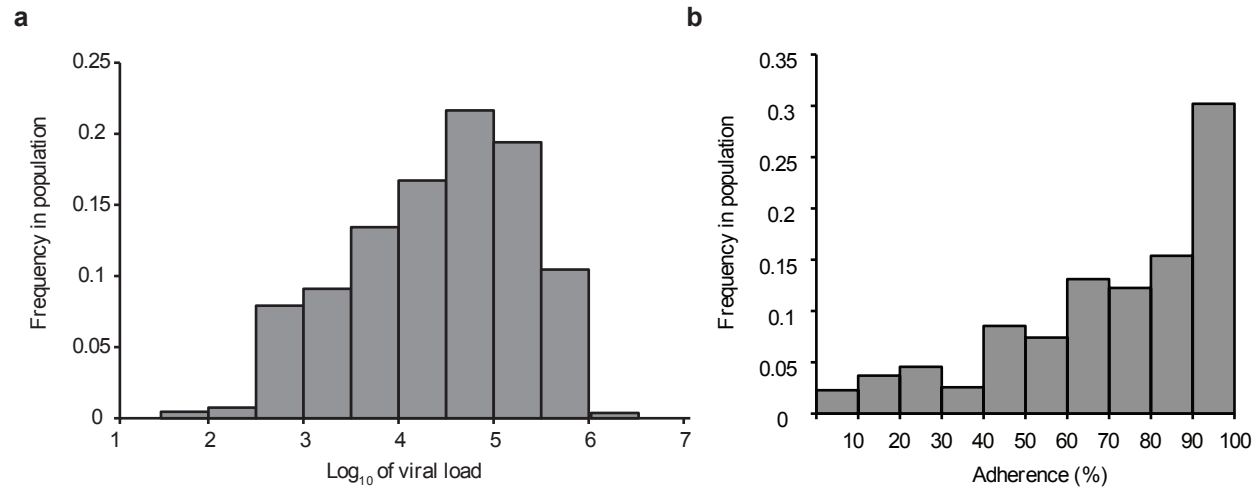

Figure 2: Distribution of a) viral load setpoints[86] (data available at www.hiv.lanl.gov/content/immunology) and b) adherence levels[30] used in simulations.

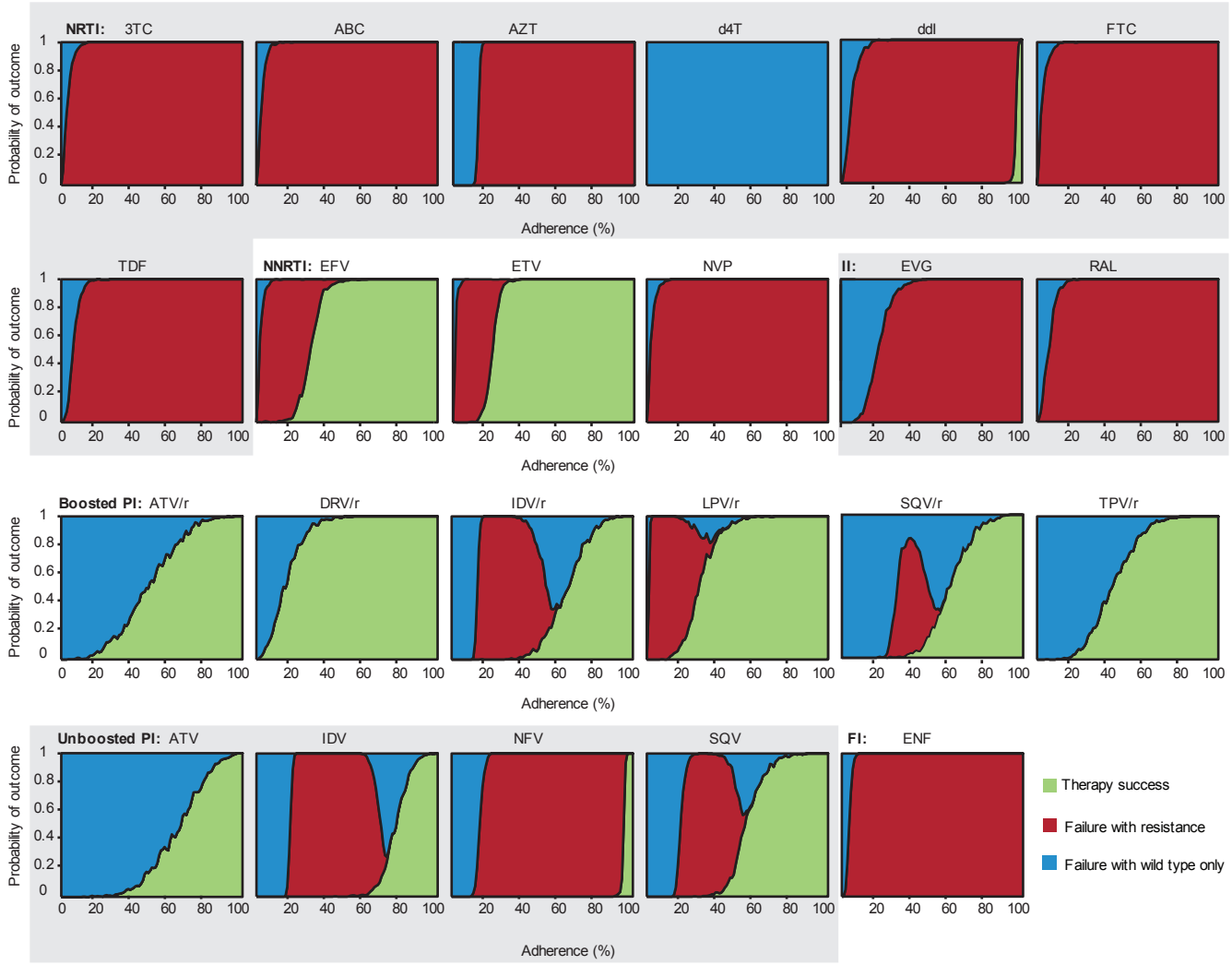

Figure 3: Simulated clinical outcomes versus adherence for all drugs. In "Suppression" trials, patients begin with a realistic distribution of treatment-naive viral loads (between 3000 and 10^6 c/mL) and undergo monotherapy for a full 48 weeks. Virologic failure (VF) is defined as a viral load above 50 c/ml at week 48. VF is classified as "via resistance" if at least 20% of the viral population at the time of detection is mutant. Adherence (x-axis) is measured as the fraction of scheduled doses taken. The height of the area shaded indicates probability of the corresponding outcome at that adherence level. 3TC, lamivudine; ABC, abacavir; AZT, zidovudine; d4T, stavudine; ddI, didanosine, FTC, emtricitabine; TDF, tenofovir disoproxil fumarate; EFV, efavirenz; ETV, etravirine; NVP, nevirapine; ATV, atazanavir; DRV, darunavir; IDV, indinavir; LPV, lopinavir; NFV, nelfinavir; SQV, saquinavir; TPV, tipranavir; EVG, elvitegravir; RAL, raltegravir; ENF, enfuvirtide.

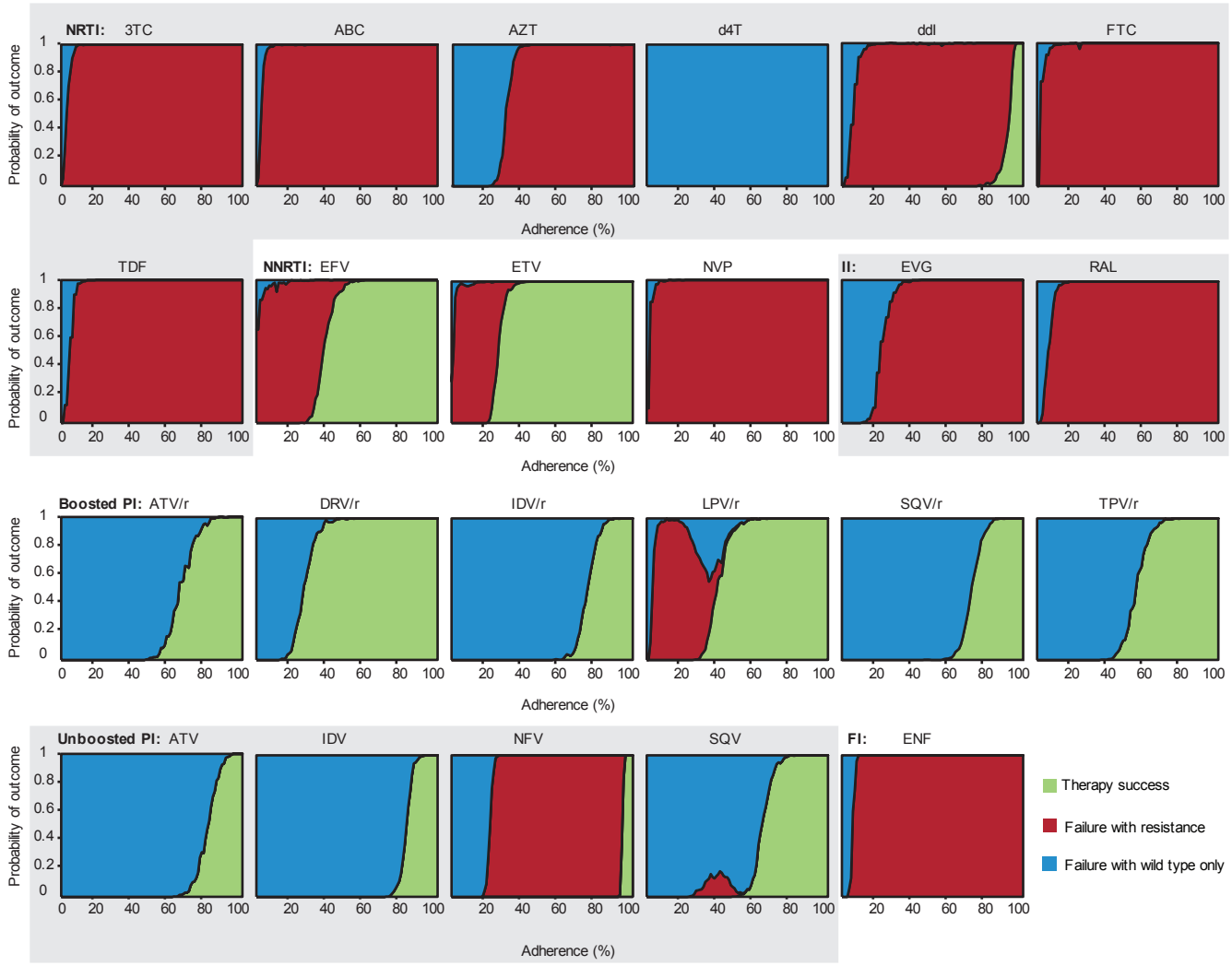

Figure 4: Simulated clinical outcomes versus adherence for all drugs. In "Maintenance" trials, patients begin with full viral suppression and undergo monotherapy for 48 weeks or until virologic failure (VF), whichever occurs first. VF is defined as "confirmed rebound": two consecutive weekly measurements (starting at week 5) with viral load above 200 c/mL. VF is classified as "via resistance" if at least 20% of the viral population at the time of detection is mutant. Adherence (x-axis) is measured as the fraction of scheduled doses taken. The height of the area shaded indicates probability of the corresponding outcome at that adherence level.

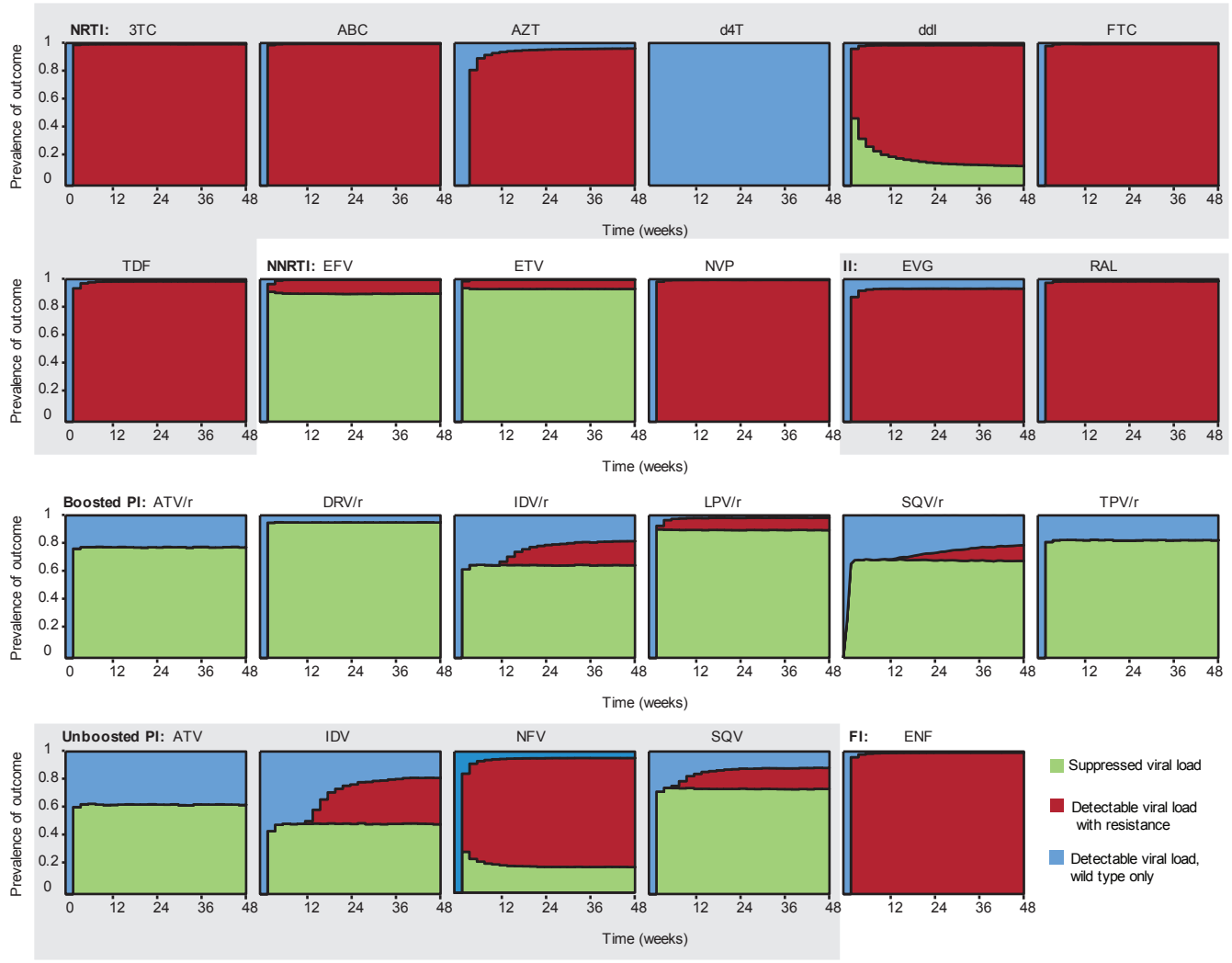

Figure 5: Simulated clinical outcomes versus time for all drugs. In "Suppression" trials, patients begin with a realistic distribution of treatment-naive viral loads (between 3000 and 10^6 c/mL) and undergo monotherapy for a variable time (x-axis). "Detectable viral load" is defined as above 50 c/ml and is classified as "via resistance" if at least 20% of the viral population at the time of detection is mutant. The height of the area shaded indicates prevalence of the corresponding outcome at that time. Patients have a realistic distribution of adherence levels with an average of 70%.

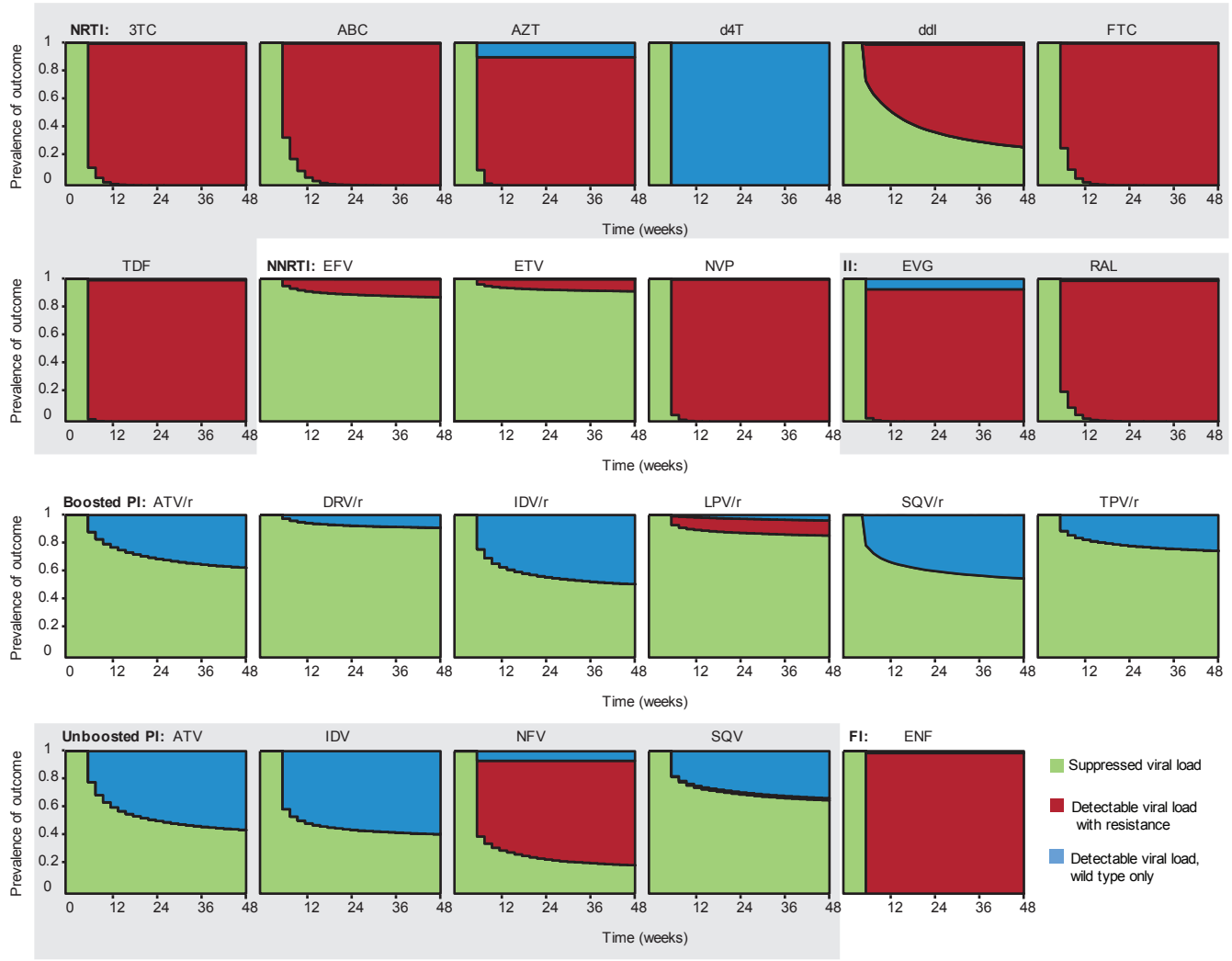

Figure 6: Simulated clinical outcomes versus time for all drugs. In "Maintenance" trials, patients begin the trial with full viral suppression and undergo monotherapy for a variable amount of time (x-axis) or until "detectable viral load" is observed, whichever occurs first. "Detectable viral load" is defined as "confirmed rebound": two consecutive weekly measurements (starting at week 5) above 200 c/mL. It is classified as "via resistance" if at least 20% of the viral population at the time of detection is mutant. The height of the area shaded indicates prevalence of the corresponding outcome at that time. Patients have a realistic distribution of adherence levels with an average of 70%.

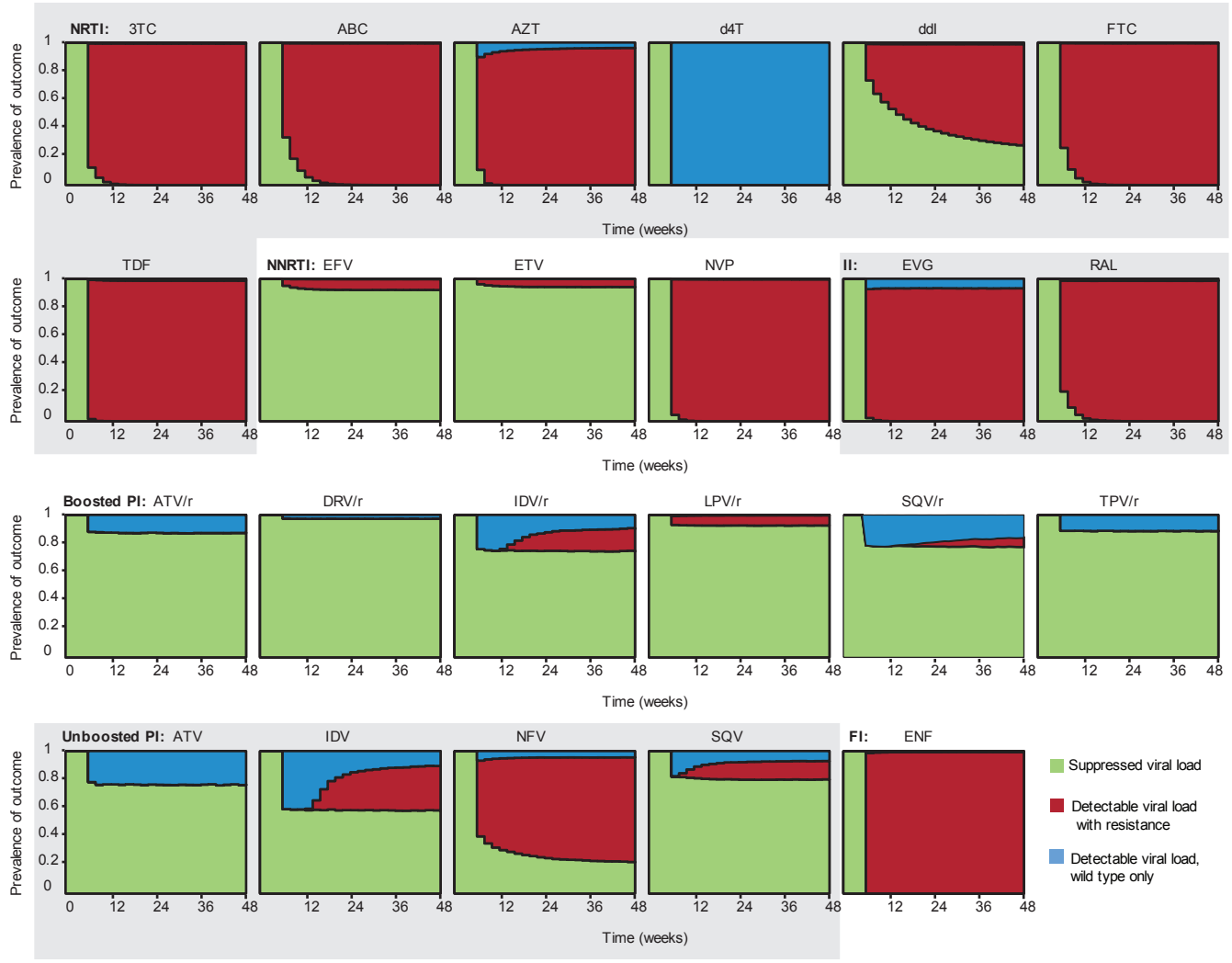

Figure 7: Simulated clinical outcomes versus time for all drugs. In "Maintenance with recovery" trials, patients begin the trial with full viral suppression and undergo monotherapy for a variable amount of time (x-axis). "Detectable viral load" is defined as "confirmed rebound": two consecutive weekly measurements (starting at week 5) with viral load above 200 c/mL. It is classified as "via resistance" if at least 20% of the viral population at the time of detection is mutant. We allow recovery, meaning that patients stay in the trial to see if they will re-suppress, instead of being removed immediately like in regular "Maintenance" trials. The height of the area shaded indicates prevalence of the corresponding outcome at that time-point. Patients have a realistic distribution of adherence levels with an average of 70%.

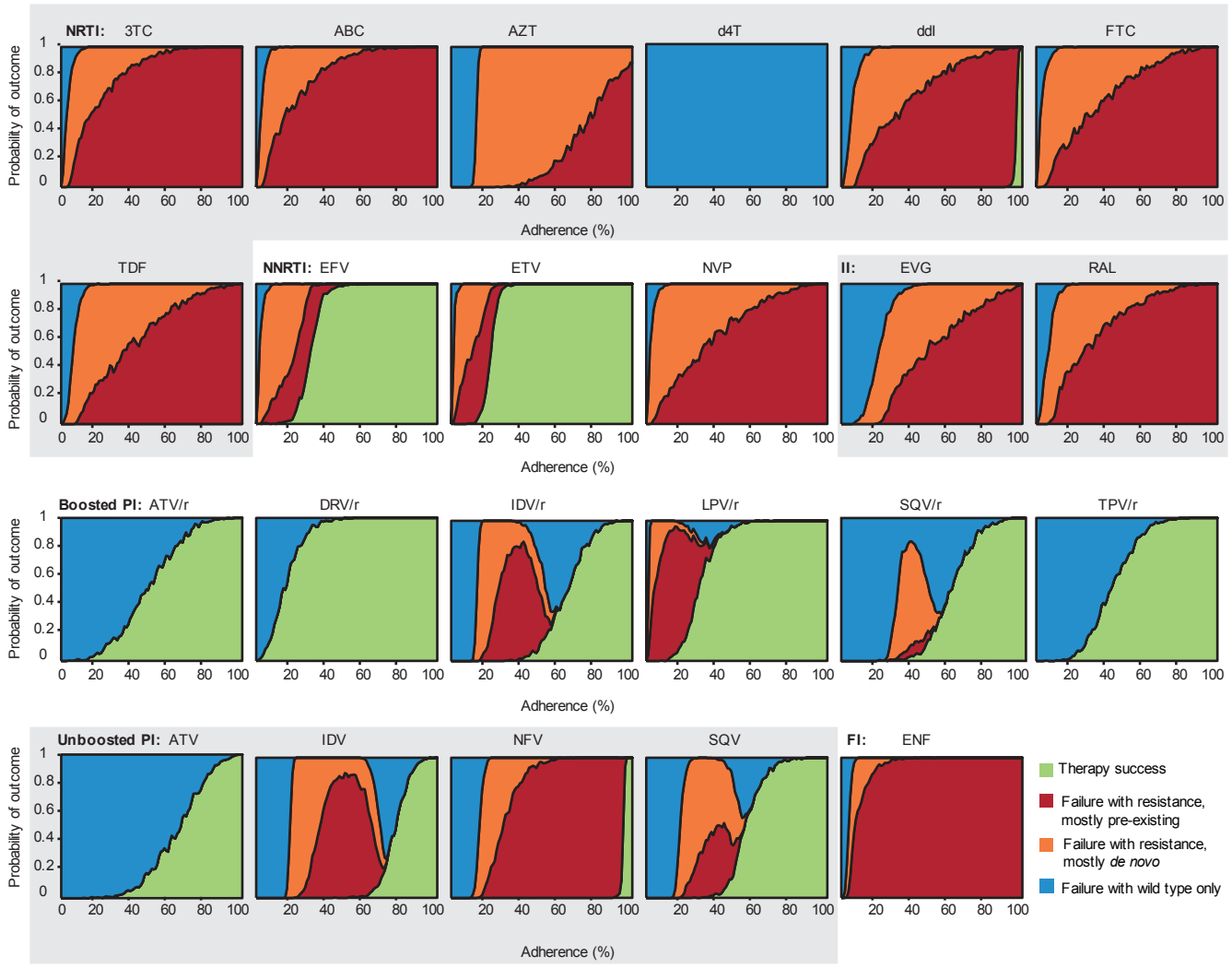

Figure 8: Simulated clinical outcomes versus adherence for all drugs, distinguishing pre-existing from *de novo* mutations. In the "Suppression" trials shown, patients begin with a realistic distribution of treatment-naive viral loads (between 3000 and 10^6 c/mL) and undergo monotherapy for a full 48 weeks. Virologic failure (VF) is defined as a viral load above 50 c/ml at week 48. VF is classified as "via resistance" if at least 20% of the viral population at the time of detection is mutant. Resistance is classified as *de novo* if the majority of mutants at the time of failure descended from a mutation event that occurred during replication since the start of the trial. Otherwise, resistance is classified as "pre-existing," which includes mutants arising from both the pre-treatment plasma population and the latent reservoir. Adherence (x-axis) is measured as the fraction of scheduled doses taken. The height of the area shaded indicates probability of the corresponding outcome at that adherence level.

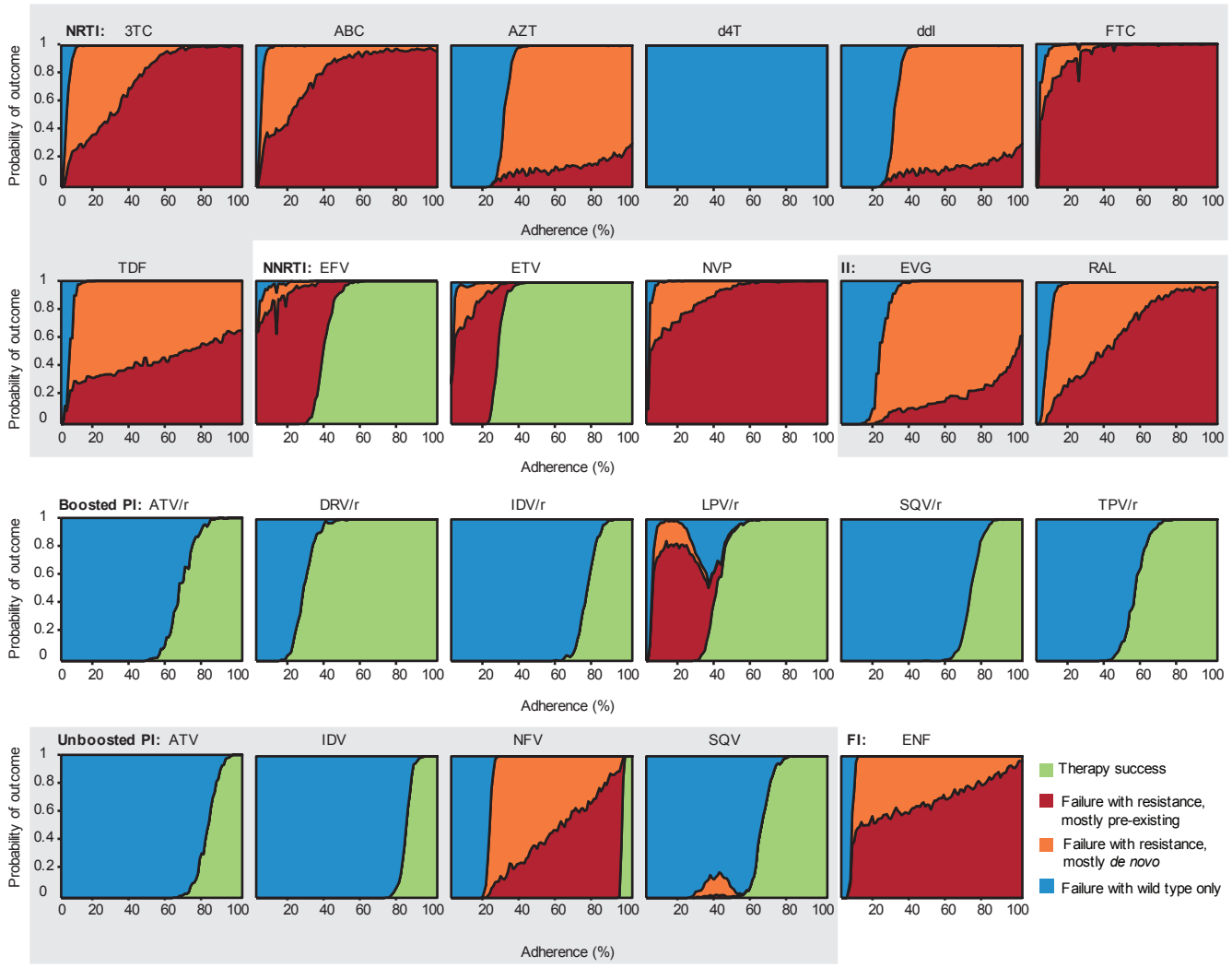

Figure 9: Simulated clinical outcomes versus adherence for all drugs, distinguishing pre-existing from *de novo* mutations. In the "Maintenance" trials shown, patients begin with full viral suppression and undergo monotherapy for 48 weeks or until virologic failure (VF), whichever occurs first. VF is defined as "confirmed rebound": two consecutive weekly measurements (starting at week 5) with viral load above 200 c/mL. VF is classified as "via resistance" if at least 20% of the viral population at the time of detection is mutant. Resistance is classified as *de novo* if the majority of mutants at the time of failure descended from a mutation event that occurred during replication since the start of the trial. Otherwise, resistance is classified as "pre-existing," which includes mutants arising from both the pre-treatment plasma population and the latent reservoir. Adherence (x-axis) is measured as the fraction of scheduled doses taken. The height of the area shaded indicates probability of the corresponding outcome at that adherence level.

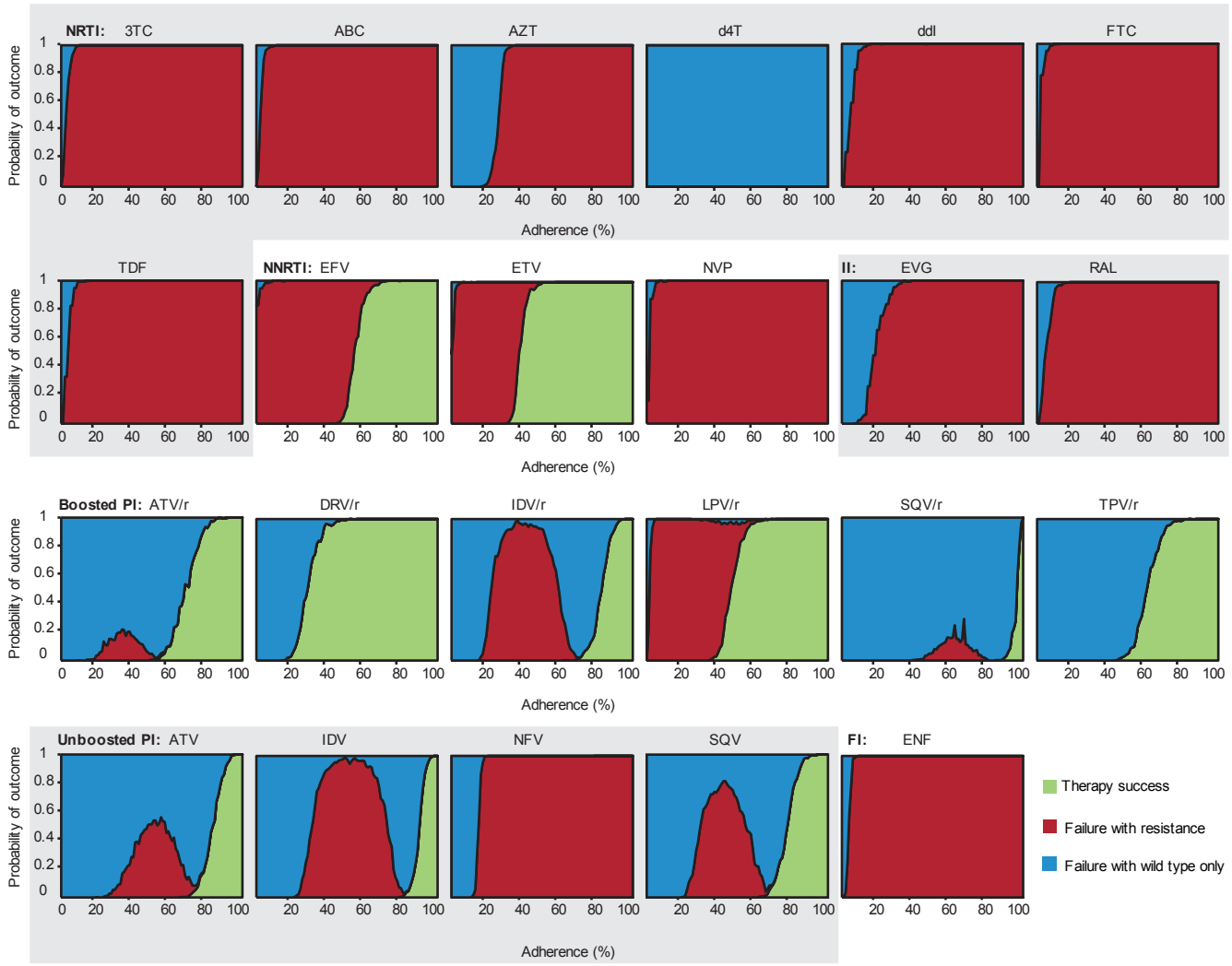

Figure 10: Simulated clinical outcomes versus adherence for all drugs, R_{00}=20. Results are shown for "Maintenance" trials only. In the "Maintenance" trials shown, patients begin with full viral suppression and undergo monotherapy for 48 weeks or until virologic failure (VF), whichever occurs first. VF is defined as "confirmed rebound": two consecutive weekly measurements (starting at week 5) with viral load above 200 c/mL. VF is classified as "via resistance" if at least 20% of the viral population at the time of detection is mutant. Adherence (x-axis) is measured as the fraction of scheduled doses taken. The height of the area shaded indicates probability of the corresponding outcome at that adherence level. As compared to R_{00}=10, increasing R_{00} to 20 leads to higher adherence levels being required for treatment success, and it extends the range of adherence levels (in both directions) for which resistant strains can cause failure. Mutant VF becomes a possible outcome for the PIs ATV, ATV/r, IDV, IDV/r, and SQV/r, and treatment success cannot occur at any adherence level for ddI and NFV.

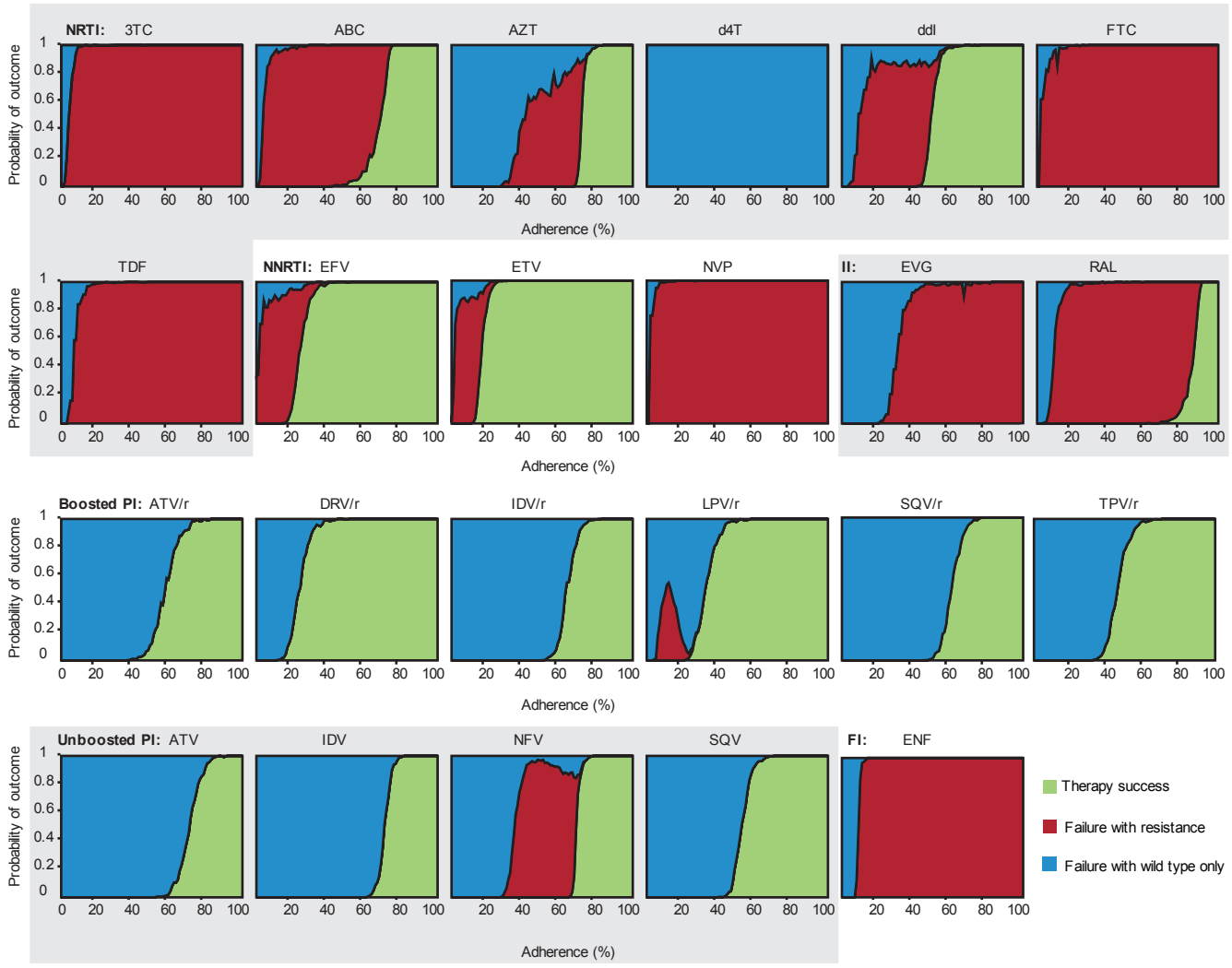

Figure 11: Simulated clinical outcomes versus adherence for all drugs, R_{00}=5. Results are shown for "Maintenance" trials only. In the "Maintenance" trials shown, patients begin with full viral suppression and undergo monotherapy for 48 weeks or until virologic failure (VF), whichever occurs first. VF is defined as "confirmed rebound": two consecutive weekly measurements (starting at week 5) with viral load above 200 c/mL. VF is classified as "via resistance" if at least 20% of the viral population at the time of detection is mutant. Adherence (x-axis) is measured as the fraction of scheduled doses taken. The height of the area shaded indicates probability of the corresponding outcome at that adherence level. As compared to R_{00}=10, decreasing R_{00} to 5 leads to lower adherence levels being required for treatment success, and it reduces the range of adherence levels for which resistant strains can cause failure. A range of high adherence levels appears where there is treatment success for ABC and AZT, and near-perfect adherence is no longer required for ddI and NFV success. Mutant VF no longer occurs for SQV, and for AZT and ddI, wild-type failure may be the first outcome to occur as adherence levels decrease from the successful range.

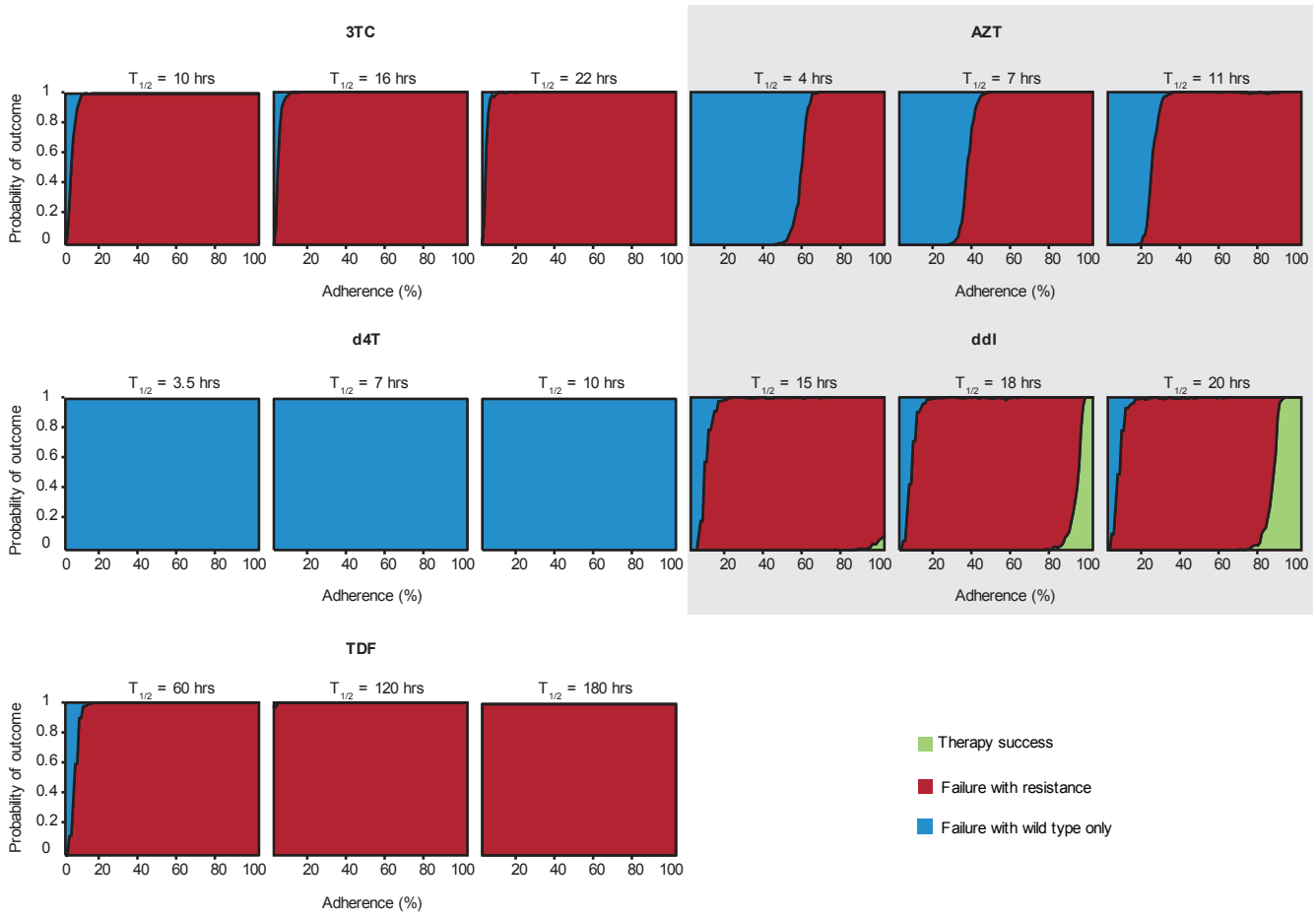

Figure 12: Simulated clinical outcomes versus adherence for NRTIs with large inter-experimental variation in half-life. The ranges included were {10, 16, 22} for 3TC, {4, 8.5, 11} for AZT, {3.5, 7, 10} for d4T, {15, 18, 20} for ddI, and {60, 120, 180} for TDF. Results are shown for "Maintenance" trials only. In the "Maintenance" trials shown, patients begin with full viral suppression and undergo monotherapy for 48 weeks or until virologic failure (VF), whichever occurs first. VF is defined as "confirmed rebound": two consecutive weekly measurements (starting at week 5) with viral load above 200 c/mL. VF is classified as "via resistance" if at least 20% of the viral population at the time of detection is mutant. Adherence (x-axis) is measured as the fraction of scheduled doses taken. The height of the area shaded indicates probability of the corresponding outcome at that adherence level. Compared to the half-lives used throughout the rest of the paper (see Suppl. Table 1), the results barely change for 3TC or d4T. For AZT, varying the half-life changes the adherence level where wild-type failure becomes more likely than mutant failure. For ddI, the adherence level where treatment success occurs shifts. For higher TDF half-lives, mutant VF becomes the only outcome, with the exception of rare ($< 3\%$) wild-type failure at the lowest adherence levels for $t_{1/2} = 120$ hours.

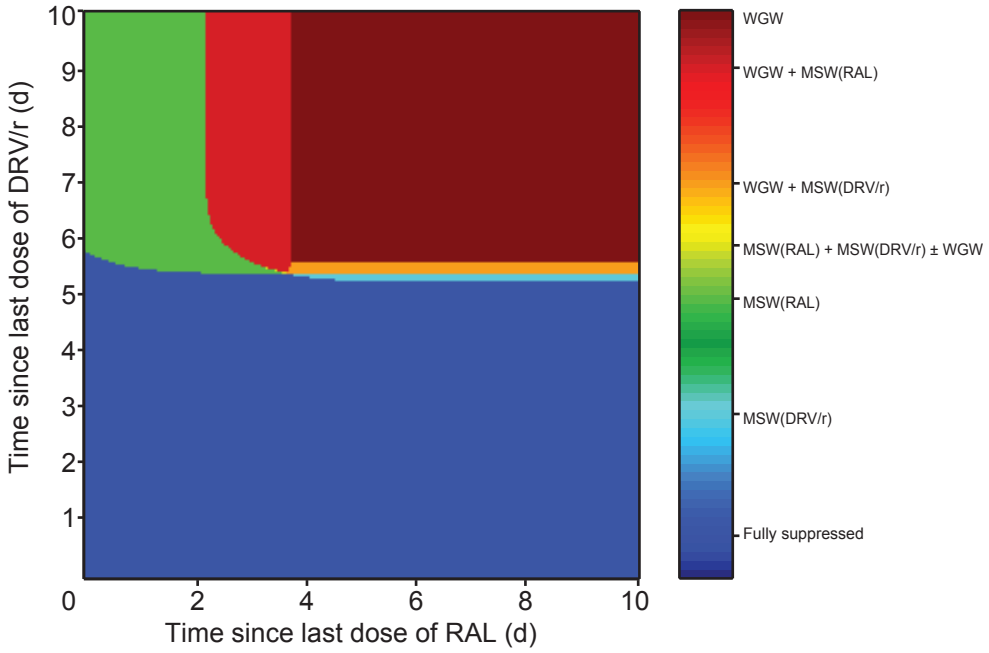

Figure 13: Selection regimes for DRV/r-RAL two-drug therapy. Depending on the length of a treatment interruption to one or both drugs, treatment may be fully suppressive or select for the wild-type strain, a mutant resistant to DRV, a mutant resistant to RAL, or combinations of these strains. The yellow region, where the MSW for both drugs overlap, is barely visible, and it is located where the other MSW regions meet, near the center of the graph.

References

[66] Markowitz, M., *et al.* A novel antiviral intervention results in more accurate assessment of human immunodeficiency virus type 1 replication dynamics and T-cell decay *in vivo*. *J. Virol.* **77**(8), 5037–5038 (2003).

[67] Little, S. J., McLean, A. R., Spina, C. A., Richman, D. D., & Havlir, D. V. Viral dynamics of acute HIV-1 infection. *J. Exp. Med.* **190**(6), 841–850 (1999).

[68] Davey, Jr., R. T., *et al.* HIV-1 and T cell dynamics after interruption of highly active antiretroviral therapy (HAART) in patients with a history of sustained viral suppression. *Proc. Natl. Acad. Sci. USA* **96**(26), 15109–15114 (1999).

[69] Ioannidis, J. P. A., *et al.* Dynamics of HIV-1 viral load rebound among patients with previous suppression of viral replication. *AIDS* **14**, 1481–1488 (2000).

[70] Krakovska, O. & Wahl, L. M. Costs versus benefits: best possible and best practical treatment regimens for HIV. *J. Math. Biol.* **54**, 385–406 (2007).

[71] Funk, G. A., *et al.* Quantification of in vivo replicative capacity of HIV-1 in different compartments of infected cells. *J. Acquir. Immune Defic. Syndr.* **26**(5), 397–404 (2001).

[72] Putter, H., Heisterkamp, S. H., Lange, J. M. A., & de Wolf, F. A Bayesian approach to parameter estimation in HIV dynamical models. *Statist. Med.* **21**(15), 2199–2214 (2002).

[73] Dinoso, J. B., *et al.* Treatment intensification does not reduce residual HIV-1 viremia in patients on highly active antiretroviral therapy. *Proc. Natl. Acad. Sci. USA* **106**(23), 9403 (2009).

[74] Hockett, R. D., *et al.* Constant mean viral copy number per infected cell in tissues regardless of high, low, or undetectable plasma HIV RNA. *J. Exp. Med.* **189**(10), 1545–1554 (1999).

[75] De Boer, R. J., Ribeiro, R. M., & Perelson, A. S. Current estimates for HIV-1 production imply rapid viral clearance in lymphoid tissues. *PLoS Comput. Biol.* **6**(9), e1000906 (2010).

[76] Sedaghat, A., Siliciano, R. F., & Wilke, C. O. Low-level HIV-1 replication and the dynamics of the resting CD4+ T cell reservoir for HIV-1 in the setting of HAART. *BMC Inf. Dis.* **8**(1), 2 (2008).

[77] Mansky, L. M. & Temin, H. M. Lower *in vivo* mutation rate of human immunodeficiency virus type 1 than that predicted from the fidelity of purified reverse transcriptase. *J. Virol.* **69**(8), 5087–5094 (1995).

[78] Abram, M. E., Ferris, A. L., Shao, W., Alvord, W. G., & Hughes, S. H. Nature, position, and frequency of mutations made in a single cycle of HIV-1 replication. *J. Virol.* **84**, 9864–9878 (2010).

[79] Kuiken, C., *et al.*, editors. *HIV Sequence Compendium 2010*. Theoretical Biology and Biophysics Group, Los Alamos National Laboratory, NM (2010).

[80] Achaz, G., *et al.* A robust measure of HIV-1 population turnover within chronically infected individuals. *Mol. Biol. Evol.* **21**(10), 1902–1912 (2004).

[81] Frost, S. D., Nijhuis, M., Schuurman, R., Boucher, C. A., & Leigh Brown, A. J. Evolution of lamivudine resistance in human immunodeficiency virus type 1-infected individuals: the relative roles of drift and selection. *J. Virol.* **74**(14), 6262–6268 (2000).

[82] Kouyos, R. D., Althaus, C. L., & Bonhoeffer, S. Stochastic or deterministic: what is the effective population size of HIV-1? *Trends Microbiol.* **14**(12), 507–511 (2006).

[83] Hill, A. L., Rosenbloom, D. I. S., & Nowak, M. A. Evolutionary dynamics of HIV at multiple spatial and temporal scales. *J. Mol. Med.* **90**, 543–561 (2012).

[84] Pennings, P. S. Standing genetic variation and the evolution of drug resistance in HIV. *PLoS Comp. Bio.* **8**(6), e1002527 (2012).

[85] Kaplan, E. L. & Meier, P. Nonparametric estimation from incomplete observations. *J. Amer. Statist. Assoc.* **53**(282), 457–481 (1958).

[86] Kiepiela, P., *et al.* Dominant influence of HLA-B in mediating the potential co-evolution of HIV and HLA. *Nature* **432**(7018), 769775 (2004).